The Interaction of C_{60}, C_{70}, and $C_{60}(CN)_2$ Radical Anions with Cobalt(II) Tetraphenylporphyrin in Solid Multicomponent Complexes

Dmitri V. Konarev,*[a, b] Salavat S. Khasanov,[a, c] Gunzi Saito,*[a] Rimma N. Lyubovskaya,[b] Yukihiro Yoshida,[a] and Akihiro Otsuka[a, d]

Abstract: A method for the synthesis of the multicomponent ionic complexes: $[Cr^{I}(C_6H_6)_2^{\bullet+}][Co^{II}(tpp)(fullerene)^{-}]\cdot C_6H_4Cl_2$, comprising bis(benzene)chromium ($Cr(C_6H_6)_2$), cobalt(II) tetraphenylporphyrin ($Co^{II}(tpp)$), fullerenes (C_{60}, $C_{60}(CN)_2$, and C_{70}), and *o*-dichlorobenzene ($C_6H_4Cl_2$) has been developed. The monoanionic state of the fullerenes has been proved by optical absorption spectra in the UV/vis/NIR and IR ranges. The crystal structures of the ionic $[\{Cr^{I}(C_6H_6)_2\}^{\bullet+}]_{1.7}[\{Co^{II}(tpp)(C_{60})\}_2]^{1.7-}\cdot 3.3\,C_6H_4Cl_2$ and $[\{Cr^{I}(C_6H_6)_2\}^{\bullet+}]_2[Co^{II}(tpp)\{C_{60}(CN)_2\}][C_{60}(CN)_2^{\bullet-}])\cdot 3\,C_6H_4Cl_2$ are presented. The essentially shortened Co···C(fullerene) bond lengths of 2.28–2.32 Å in these complexes indicate the formation of *σ*-bonded $[Co^{II}(tpp)][fullerene]^{-}$ anions, which are diamagnetic. All the ionic complexes are semiconductors with room temperature conductivity of $2\times10^{-3}-4\times10^{-6}\,S\,cm^{-1}$, and their magnetic susceptibilities show Curie–Weiss behavior. The neutral complexes of $Co^{II}(tpp)$ with C_{60}, $C_{60}(CN)_2$, C_{70}, and $Cr^{0}(C_6H_6)_2$, as well as the crystal structures of $[Co^{II}(tpp)](C_{60})\cdot 2.5\,C_6H_4Cl_2$, $[Co^{II}(tpp)](C_{70})\cdot 1.3\,CHCl_3\cdot 0.2\,C_6H_6$, and $[Cr^{0}(C_6H_6)_2][Co^{II}(tpp)]$ are discussed. In contrast to the ionic complexes, the neutral ones have essentially longer Co···C(fullerene) bond lengths of 2.69–2.75 Å.

Keywords: crystal engineering · donor–acceptor systems · fullerenes · porphyrinoids · solid-state structures

Introduction

Ionic charge-transfer (CT) complexes and salts based on fullerenes[1] show intriguing physical properties.[2–6] The compounds obtained up to now involve strong organic and organometallic donors (denoted as D_1), namely, metallocenes $Co^{II}(Cp)_2$,[7, 8] $Cr^{0}(C_6H_6)_2$,[9] $Cr^{0}(C_6H_5Me)_2$,[9, 10] $Cr^{0}(C_6H_3Me_3)_2$,[9] $Ni^{II}(Cp^*)_2$,[11] $Co^{II}(Cp^*)_2$,[12] $Cr^{II}(Cp^*)_2$,[13] and $Fe^{I}(Cp)(C_6Me_6)$;[14] metalloporphyrinates $Cr^{II}(tpp)$[15] and $Sn^{II}TpTP$;[8] and the amine TDAE.[16] All of these ionic compounds are two-component ones and can be presented by a general formula: $[(D_1)^{\bullet+}(fullerene)^{\bullet-}]$, some of them also contain solvent molecules (S).

At the same time, most organic and organometallic donors: substituted tetrachalcogenafulvalenes,[17–19] aromatic hydrocarbons,[19, 20] amines,[21] porphyrins,[22, 23] porphyrazines,[24] and their metal-containing analogues[22, 23, 25–28] (denoted as D_2) yield mainly neutral complexes with fullerenes: $[(D_2)^{\delta+}(fullerene)^{\delta-}]\cdot S$, where the degree of charge transfer (δ) is close to 0. The advantage of these complexes is their

[a] Dr. D. V. Konarev, Prof. G. Saito, Dr. S. S. Khasanov, Dr. Y. Yoshida, Dr. A. Otsuka
Division of Chemistry, Graduate School of Science
Kyoto University, Sakyo-ku, Kyoto 606-8502 (Japan)
Fax: (+81) 75-753-4035
E-mail: konarev@icp.ac.ru, saito@kuchem.kyoto-u.ac.jp

[b] Dr. D. V. Konarev, Prof. R. N. Lyubovskaya
Institute of Problems of Chemical Physics RAS, Chernogolovka
Moscow Region 142432 (Russia)
Fax: (+7) 96-515-35-88

[c] Dr. S. S. Khasanov
Institute of Solid-State Physics RAS, Chernogolovka
Moscow Region, 142432 (Russia)

[d] Dr. A. Otsuka
Research Center for Materials Sciences, Kyoto University
Sakyo-ku, Kyoto, 606-8502 (Japan)

Supporting information for this article is available on the WWW under http://www.chemeurj.org or from the author.

Abbreviations in the text: $Co^{II}(Cp)_2$: cobaltocene; $Cr^{0}(C_6H_6)_2$: bis(benzene)chromium(0); $Cr^{0}(C_6H_5Me)_2$: bis(toluene)chromium(0); $Cr^{0}(C_6H_3Me_3)_2$: bis(mesitylene)chromium(0); $Ni^{II}(Cp^*)_2$: bis(pentamethylcyclopentadienyl)nickel(II); $Co^{II}(Cp^*)_2$: bis(pentamethylcyclopentadienyl)cobalt(II); $Cr^{II}(Cp^*)_2$: bis(pentamethylcyclopentadienyl)chromium(II); $Cr^{II}(tpp)$: 5,10,15,20-tetraphenyl-21*H*,23*H*-porphyrinate chromium(II); $Sn^{II}TpTP$: 5,10,15,20-tetratolyl-21*H*,23*H*-porphyrinate tin(II); TDAE: tetrakis(dimethylamino)ethylene; $Fe^{II}(Cp)_2$: ferrocene; $H_2(tpp)$: 5,10,15,20-tetraphenyl-21*H*,23*H*-porphyrin; $Zn^{II}(tpp)$: 5,10,15,20-tetraphenyl-21*H*,23*H*-porphyrinate zinc(II); $Cu^{II}(tpp)$: 5,10,15,20-tetraphenyl-21*H*,23*H*-porphyrinate copper(II); $Co^{II}(tmpp)$: 5,10,15,20-tetrakis(*p*-methoxyphenyl)-21*H*,23*H*-porphyrinate cobalt(II); $Co^{II}(tbp)$: 5,10,15,20-tetrakis[3,5-(di-*tert*-butyl)phenyl]-21*H*,23*H*-porphyrinate cobalt(II); $Co^{II}(oep)$: 2,3,7,8,12,13,17,18-octaethylporphyrinate cobalt(II); Ph_4P^{+}: tetraphenylphosphonium cation.

 DOI: 10.1002/chem.200204470

ability to form various packing motifs of fullerene molecules in a crystal. The molecular configurations and fullerene networks, which range from one- to three-dimensional in fullerene complexes with tetraphenylporphyrin and their metal-containing analogues, were demonstrated in our previous publications.[23, 26a, b, c] It is well known that the neutral complexes cannot show interesting conducting and magnetic properties, and the change of their ground state to an ionic one may be promising in the design of functional organic solids. A third component with strong donor ability introduced into the complex can ionize the fullerenes (the above-mentioned D_1 molecules) and change their ground state.

To combine D_1 and D_2 molecules in one complex with fullerene, we designed multicomponent complexes of fullerenes of a general formula $[(D_1)^{\bullet}(\text{fullerene})(D_2)]\cdot S$; here D_1 is a donor molecule of a small size potentially able to ionize fullerenes, and D_2 is a large structure-forming molecule. Tetraphenylporphyrins are convenient D_2 components since H_2(tpp) or M(tpp) (M = Co^{II}, Cu^{II}, and Zn^{II}) and fullerenes form a specific architecture with large cavities or channels,[22, 23, 26e] which can accommodate a small D_1 component. In our previous work[26e] we developed a method for the incorporation of ferrocene ($Fe^{II}Cp_2$) into [Co^{II}(tpp)(py)] and [Zn^{II}(tpp)(py)] (py: pyridine) complexes with C_{60}. The resulting $[M^{II}(tpp)(py)]_2[Fe^{II}(Cp)_2](C_{60})\cdot C_6H_5Me$ (M = Co, Zn) complexes still have a neutral ground state since $Fe^{II}(Cp)_2$ is too weak a donor to ionize C_{60}.

In contrast to $Fe^{II}(Cp)_2$, $Cr^0(C_6H_6)_2$ has essentially stronger donor properties ($E^{+/0}_{1/2} = -0.72$ V[29]) to ionize fullerenes ($E^{0/-}_{1/2}$ of C_{60} and C_{70} ~ -0.4 V[30] and $E^{0/-}_{1/2}$ of $C_{60}(CN)_2 = -0.25$ V[31]) and can form ionic CT complexes with them: $[Cr^I(C_6H_6)_2]^{\bullet+}(C_{60})^{\bullet-}$[9] and $[Cr^I(C_6H_6)_2]^{\bullet+}[C_{60}(CN)_2]^{\bullet-}\cdot C_6H_6$.[31] The size of the $Cr^0(C_6H_6)_2$ molecule is comparable with that of solvent molecules and allows this donor to be used as a D_1 component in the multicomponent ionic $[(D_1)^{\bullet+}(\text{fullerene})^-(D_2{}^0)]\cdot S$ complexes.

In this paper we present the new ionic multicomponent $[Cr^I(C_6H_6)_2]^{\bullet+}[Co^{II}(tpp)(\text{fullerene})^-]\cdot C_6H_4Cl_2$ complexes together with the neutral molecules: $[Co^{II}(tpp)](\text{fullerene})\cdot S$ (fullerene = C_{60}, $C_{60}(CN)_2$, and C_{70}; $C_6H_4Cl_2$ = *o*-dichlorobenzene; S = $C_6H_4Cl_2$, $CHCl_3$, C_6H_6, C_6H_5Me), and $[Cr^0(C_6H_6)_2][Co^{II}(tpp)]$. The complexes have been characterized by IR, UV/vis/NIR, and EPR spectroscopy, and their magnetic and transport properties have been studied. The crystal structures of $[\{Cr^I(C_6H_6)_2\}_{1.7}][\{Co^{II}(tpp)(C_{60})\}_2]\cdot 3.3\,C_6H_4Cl_2$ (**1**), $[\{Cr^I(C_6H_6)_2\}_2][Co^{II}(tpp)\{C_{60}(CN)_2\}][C_{60}(CN)_2]\cdot 3\,C_6H_4Cl_2$ (**3**),[32] $[Co^{II}(tpp)](C_{60})\cdot 2.5\,C_6H_4Cl_2$ (**4**), $[Co^{II}(tpp)](C_{70})\cdot 1.3\,CHCl_3\cdot 0.2\,C_6H_6$ (**6**), and $[Cr^0(C_6H_6)_2][Co^{II}(tpp)]$ (**9**) have been solved by using single-crystal X-ray data. The interaction of Co^{II}(tpp) with neutral fullerenes C_{60}, $C_{60}(CN)_2$, and C_{70} and their radical anions in the solid complexes has been analyzed.

Results

Synthesis: The complexes **1**–**9** are listed in Table 1. The crystals of **1**–**3** were prepared under anaerobic conditions by diffusion of *n*-hexane into a solution of $Cr^0(C_6H_6)_2$, fullerene, and Co^{II}(tpp) in $C_6H_4Cl_2$. The $Cr^0(C_6H_6)_2$/fullerene/Co^{II}(tpp) molar ratio is 2:1:1. Ionic $[Cr^I(C_6H_6)_2]^{\bullet+}[\text{fullerene}]^{\bullet-}\cdot C_6H_4Cl_2$ and $[Cr^0(C_6H_6)_2][Co^{II}(tpp)]$ (**9**) were crystallized in the presence of an excess of $Cr^0(C_6H_6)_2$ (4:1:1 molar ratio). H_2(tpp), Cu^{II}(tpp), Zn^{II}(tpp) (as a D_2 component), or bulky $Cr^{II}(Cp^*)_2$[#] ■■ (as a D_1 component) do not form multicomponent complexes with C_{60}.

Crystal structures: The main building block of $[\{Cr^I(C_6H_6)_2\}_{1.7}][\{Co^{II}(tpp)(C_{60})\}_2]\cdot 3.3\,C_6H_4Cl_2$ (**1**) is the $[Co^{II}(tpp)(C_{60})]$ unit (Figure 1a). There are two $[Co^{II}(tpp)(C_{60})]$ units (**A** and **B**), which have different atomic displacement parameters for the fullerene moieties and Co···C(C_{60}) bond lengths of 2.294(10) Å in unit **A** and 2.319(9) Å in unit **B**. The next shortened Co···C(C_{60}) contacts for carbon atoms closest to coordinated carbon are 3.004–3.204 Å (inset, Figure 1a). Such a coordination corresponds to the σ bonding of Co^{II}(tpp) to C_{60}. The N(Co^{II}(tpp))···C(C_{60}) bond lengths are 2.968–3.264 Å in both units.

The supramolecular arrangement of **1** is shown in Figure 2. The σ-bonded $[Co^{II}(tpp)(C_{60})]$ units form a cage structure

Table 1. Data for crystals of **1**–**9**.

N	Complex	Elemental analysis found/calcd				Shape
		C [%]	H [%]	N [%]	Cl [%]	
1	$[\{Cr^I(C_6H_6)_2\}_{1.7}][\{Co^{II}(tpp)(C_{60})\}_2]\cdot 3.3\,C_6H_4Cl_2$[a]	according to X-ray diffraction data				elongated prisms
2	$[\{Cr^I(C_6H_6)_2\}_2][Co^{II}(tpp)(C_{70})](C_{70})\cdot 2\,C_6H_4Cl_2$[b]	84.48/84.62	2.16/2.16	2.63/2.03	5.12/5.08	prisms
3	$[\{Cr^I(C_6H_6)_2\}_2][Co^{II}(tpp)\{C_{60}(CN)_2\}][C_{60}(CN)_2]\cdot 3\,C_6H_4Cl_2$[c]	according to X-ray diffraction data				elongated parallelepipeds
4	$[Co^{II}(tpp)](C_{60})\cdot 2.5\,C_6H_4Cl_2$	according to X-ray diffraction data				prisms
5	$[Co^{II}(tpp)](C_{60})\cdot C_6H_5Me$	89.55/89.76	2.57/2.42	3.84/3.77	–	prisms
6	$[Co^{II}(tpp)](C_{70})\cdot 1.3\,CHCl_3\cdot 0.2\,C_6H_6$	according to X-ray diffraction data				prisms
7	$[Co^{II}(tpp)](C_{70})\cdot 2.5\,C_6H_4Cl_2$	82.40/82.44	1.90/2.02	3.00/2.97	9.21/9.44	elongated plates
8	$[Co^{II}(tpp)]\{C_{60}(CN)_2\}\cdot 2.5\,C_6H_5Me\cdot 1.5\,CHCl_3$	80.40/80.79	2.44/2.40	4.62/4.70	8.78/8.64	prisms
9	$[Cr^0(C_6H_6)_2][Co^{II}(tpp)]$	according to X-ray diffraction data				parallelepipeds

The atomic ratio from the data of microprobe analysis (Co/Cr/Cl): obs/calcd: [a] $1.00\pm0.07:0.86\pm0.07:2.2\pm0.1$ / 1:0.85:3.3. [b] $1.00\pm0.07:1.96\pm0.07:4.1\pm0.1$ / 1:2:4. [c] $1.00\pm0.07:2.00\pm0.07:6.4\pm0.1$ / 1:2:6.

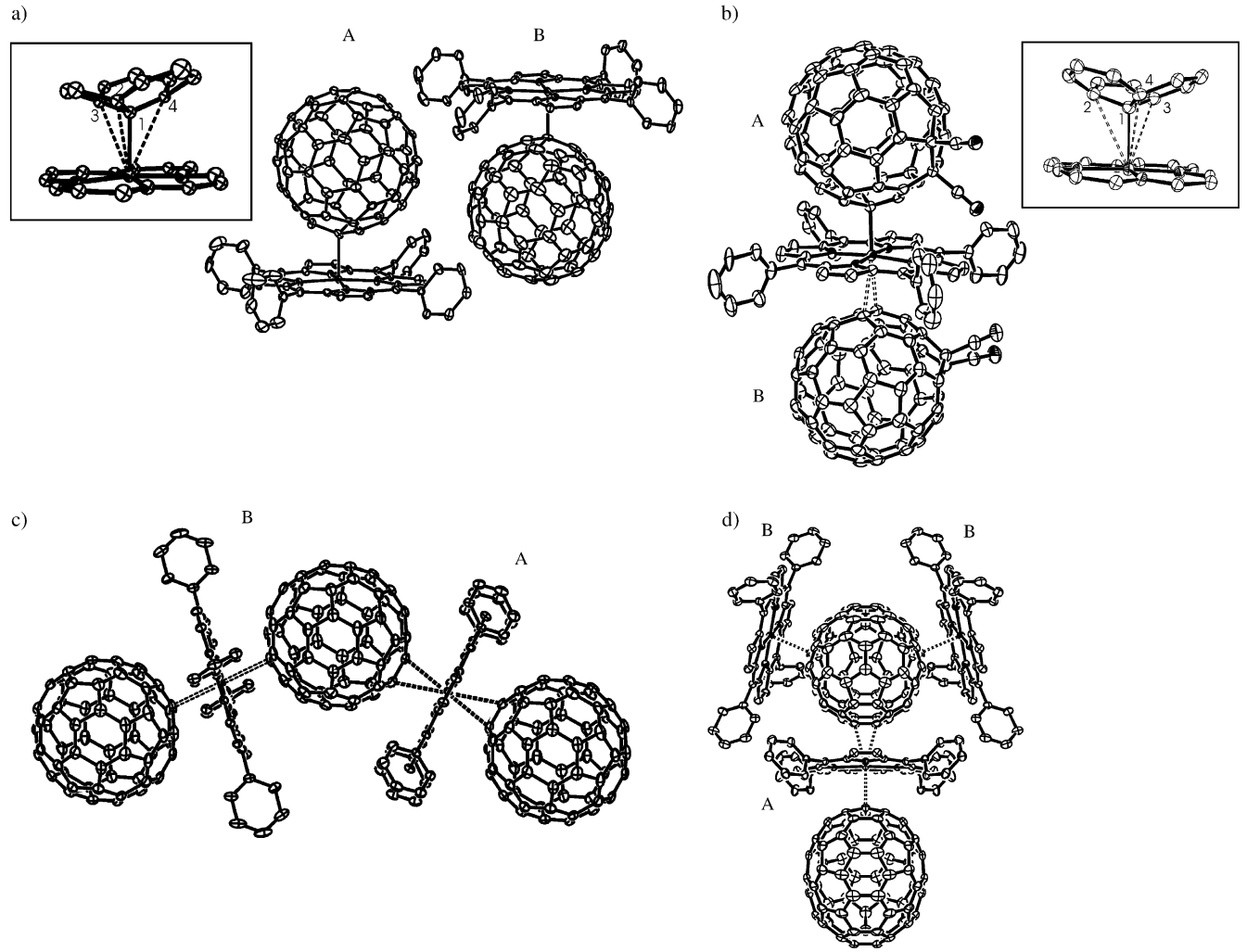

Figure 1. Different types of fullerene/porphyrin interaction in: a) $[\{Cr^{I}(C_6H_6)_2\}_{1.7}][\{Co^{II}(tpp)(C_{60})\}_2]\cdot 3.3\,C_6H_4Cl_2$ (**1**). Inset: a detailed view of the Co···C σ bond in $[Co^{II}(tpp)(C_{60})]$ unit "A" (the Co···C(n) lengths are $n=1$: 2.29, $n=2$: 3.00, $n=3$: 3.00, $n=4$: 3.20 Å. b) $[\{Cr^{I}(C_6H_6)_2\}_2][Co^{II}(tpp)\{C_{60}(CN)_2\}]$-$[C_{60}(CN)_2]\cdot 3\,C_6H_4Cl_2$ (**3**). Inset: a detailed view of the Co···C σ bond in $[Co^{II}(tpp)(C_{60})(CN)_2]$ unit (the Co···C(n) lengths are $n=1$: 2.28, $n=2$: 3.09, $n=3$: 3.06, $n=4$: 2.99 Å. c) $[Co^{II}(tpp)](C_{60})\cdot 2.5\,C_6H_4Cl_2$ (**4**). d) $[Co^{II}(tpp)](C_{70})\cdot 1.3\,CHCl_3\cdot 0.2\,C_6H_6$ (**6**). The shortened van der Waals contacts (<3.0 Å) and the σ bonding are shown by dashed and full lines, respectively.

with large cavities connected through channels along the *b* axis. The walls of each cavity are built of six $[Co^{II}(tpp)(C_{60})]$ units. The cavities accommodate both $C_6H_4Cl_2$ and $Cr^{I}(C_6H_6)_2$ in six crystallographically different positions. Three of them are partially occupied by orientationally disordered $C_6H_4Cl_2$, one position is partially occupied by orientationally disordered $Cr^{I}(C_6H_6)_2$, and the last two neighboring positions are shared by both $Cr^{I}(C_6H_6)_2$ and $C_6H_4Cl_2$. The fullerene molecules form isolated pairs with a center-to-center bond length of 10.16 Å and a shortened C···C contact of 3.216 Å. $[\{Cr^{I}(C_6H_6)_2\}_2][Co^{II}(tpp)\{C_{60}(CN)_2\}][C_{60}(CN)_2]\cdot 3\,C_6H_4Cl_2$ (**3**) contains $[Co^{II}(tpp)][\{C_{60}(CN)_2\}_2]$ units (Figure 1b). One $C_{60}(CN)_2$ (**A**) has a σ-type coordination to $Co^{II}(tpp)$ with the shortest Co···C bond length being 2.283(3) Å. The shortened Co···C contacts for carbon atoms closest to coordinated carbon are 2.99–3.09 Å (inset, Figure 1b). The second $C_{60}(CN)_2$ molecule (**B**) forms only shortened van der Waals contacts with $Co^{II}(tpp)$ of the η^2-type with Co···C distances of 2.790(3) and 2.927(3) Å.

The packing of **3** is shown in Figure 3. The $[Co^{II}(tpp)][\{C_{60}(CN)_2\}_2]$ units form a cage structure with channels (**I** and **II**) arranged along the *a* axis. **I** is occupied by ordered $Cr^{I}(C_6H_6)_2$ molecules. Each $Cr^{I}(C_6H_6)_2$ is surrounded by six $C_{60}(CN)_2$ molecules among which four molecules ($2\,\mathbf{A}+2\,\mathbf{B}$) project C≡N groups toward one $Cr^{I}(C_6H_6)_2$ and the other two molecules ($2\,\mathbf{B}$) toward the $Cr^{I}(C_6H_6)_2$ embedded in the neighboring channels **I.** The $N(C_{60}(CN)_2)\cdots C(Cr^{I}(C_6H_6)_2)$ contacts are 3.24–3.26 Å. Channel **II** is larger than **I** since its walls contain two additional ordered $Cr^{I}(C_6H_6)_2$, which form the shortened $C(C_{60})\cdots C(Cr^{I}(C_6H_6)_2)$ contacts of 3.38–3.44 Å. Channel **II** contains disordered $Cr^{I}(C_6H_6)_2$ and $C_6H_4Cl_2$ (not depicted in Figure 3) in two crystallographically independent positions. One of these positions is occupied only by $C_6H_4Cl_2$ and the other one is shared by both $Cr^{I}(C_6H_6)_2$ and $C_6H_4Cl_2$. Their disorder is associated with the absence of shortened contacts with fullerenes. In **3** the fullerene molecules form several shortened C···C contacts to each other (3.17–3.38 Å).

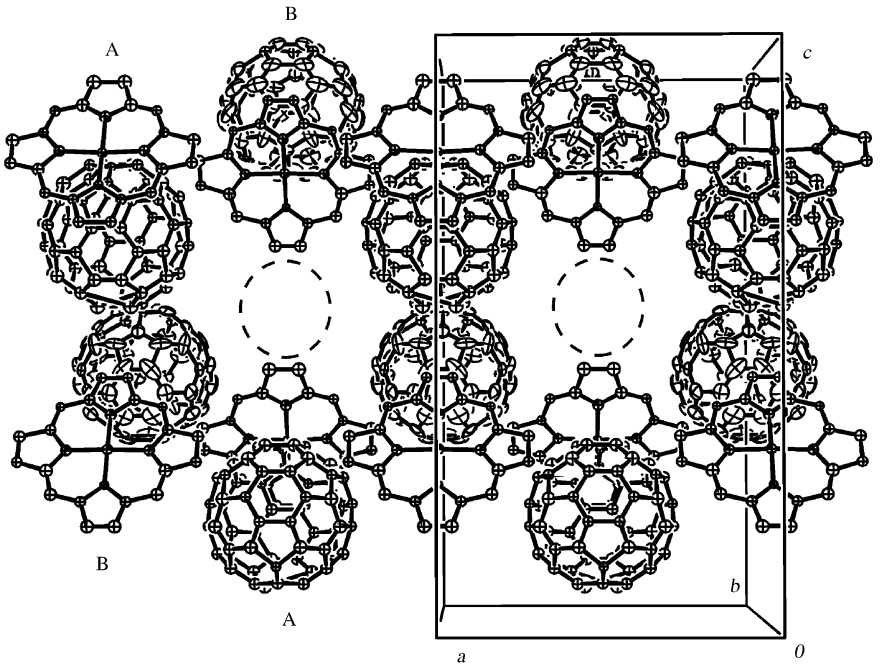

Figure 2. The supramolecular arrangement of $[\{Cr^{I}(C_6H_6)_2\}_{1.7}][\{Co^{II}(tpp)(C_{60})\}_2]\cdot 3.3\,C_6H_4Cl_2$ (**1**) (view along the *b* axis). The cavities connected by the through channels are shown by dashed circles. The phenyl substituents of the Co^{II}(tpp), $Cr^{I}(C_6H_6)_2$ and $C_6H_4Cl_2$ moieties are omitted.

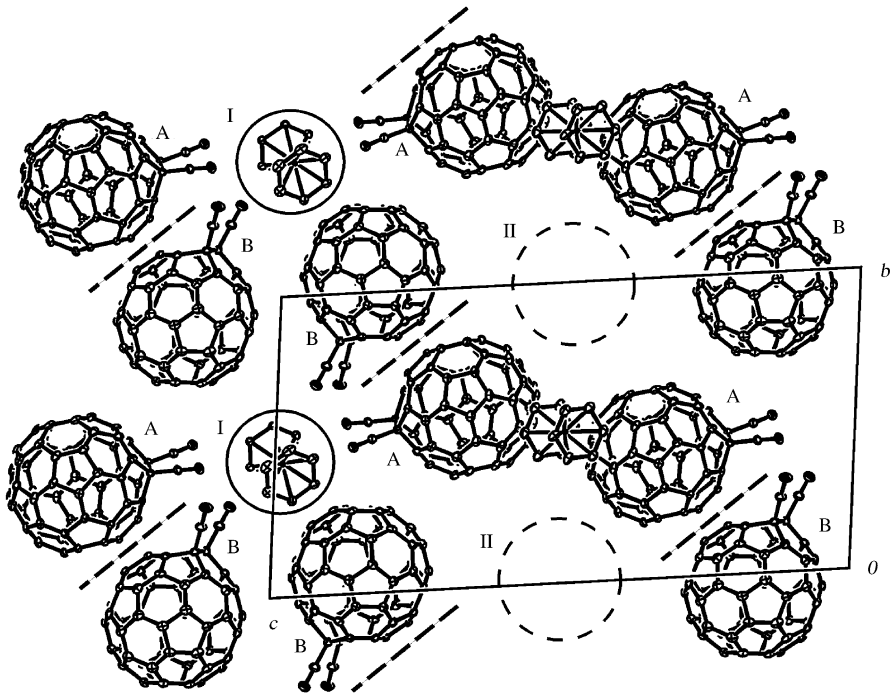

Figure 3. The two types of channel in $[\{Cr^{I}(C_6H_6)_2\}_2][Co^{II}(tpp)\{C_{60}(CN)_2\}][C_{60}(CN)_2]\cdot 3\,C_6H_4Cl_2$ (**3**) (view along the channels). The channels **I** and **II** are depicted by full and dashed circles, respectively. The positions of the Co^{II}(tpp) macrocycles are shown schematically by dashed lines.

$[Co^{II}(tpp)](C_{60})\cdot 2.5\,C_6H_4Cl_2$ (**4**) is isostructural to $H_2(tpp)\cdot C_{60}\cdot(C_6H_5Me)_3$,[22] $[Zn^{II}(tpp)](C_{70})$,[22] and $[Cu^{II}(tpp)](C_{70})\cdot 1.5\,C_6H_5Me\cdot 0.5\,C_2HCl_3$.[23]

The main structural motif of the complex is zigzag chains of alternating Co^{II}(tpp) and C_{60} molecules (Figures 1*c* and 4). Each C_{60} molecule forms shortened contacts with the two $[Co^{II}(tpp)]$ units (**A** and **B**). The dihedral angle between the planes of porphyrin macrocycles of **A** and **B** is 44.1°. **A** forms shortened van der Waals Co⋯C (C_{60}) contacts (2.691(3) and 2.796(3) Å) of the η^2 type with the 6–6 bond of C_{60}, while **B** forms only one shortened Co⋯C (C_{60}) contact of 2.690(3) Å (the Co⋯C(C_{60}) contact with another carbon atom of this 6–6 bond is 3.11 Å). There are also several shortened N(Co^{II}(tpp))⋯C(C_{60}) contacts in the 2.95–3.37 Å range. The zigzag arrangement of C_{60} and Co^{II}(tpp) molecules in the chains affords large cavities (Figure 4, dashed circles) occupied by phenyl substituents of Co^{II}(tpp) and $C_6H_4Cl_2$. Each C_{60} molecule in **4** has two adjacent C_{60} molecules with van der Waals C⋯C contacts in the 3.11–3.36 Å range and a center-to-center distance of 10.10 Å.

$[Co^{II}(tpp)](C_{70})\cdot 1.3\,CHCl_3\cdot 0.2\,C_6H_6$ (**6**) contains C_{70} layers parallel to the mirror (010) plane of the lattice (Figure 5). There are two crystallographically independent C_{70} and Co^{II}(tpp) molecules (**A** and **B**). The saddle-shaped **A** forms shortened Co⋯C(C_{70}) contacts in the 2.70–2.90 Å range with two crystallographically independent C_{70} molecules, while the planar **B** has a shortened contact of 2.751(3) Å with only one C_{70} molecule and its crystallographic equivalent (Figure 1d). There are several shortened C⋯C contacts (3.30–3.48 Å) between the nonequivalent C_{70} molecules in the layer, so that the zigzag chains of C_{70} molecules are clearly pronounced (Figure 5). Disordered solvent molecules occupy the cavities within the C_{70} layer.

$[Cr^{0}(C_6H_6)_2][Co^{II}(tpp)]$ (9): The complex has a layered structure. An almost square network of Co^{II}(tpp) molecules in the layer contains ordered $Cr^{0}(C_6H_6)_2$ molecules in the cavities formed by the phenyl groups of Co^{II}(tpp) (Figure 6).

Conformation of Co^{II}(tpp) in the complexes: The main geometric parameters of porphyrin macrocycles for **1**, **3**, **4**, **6**, **9** and related compounds are presented in Table 2. The values of bond lengths and angles in the porphyrin ligand

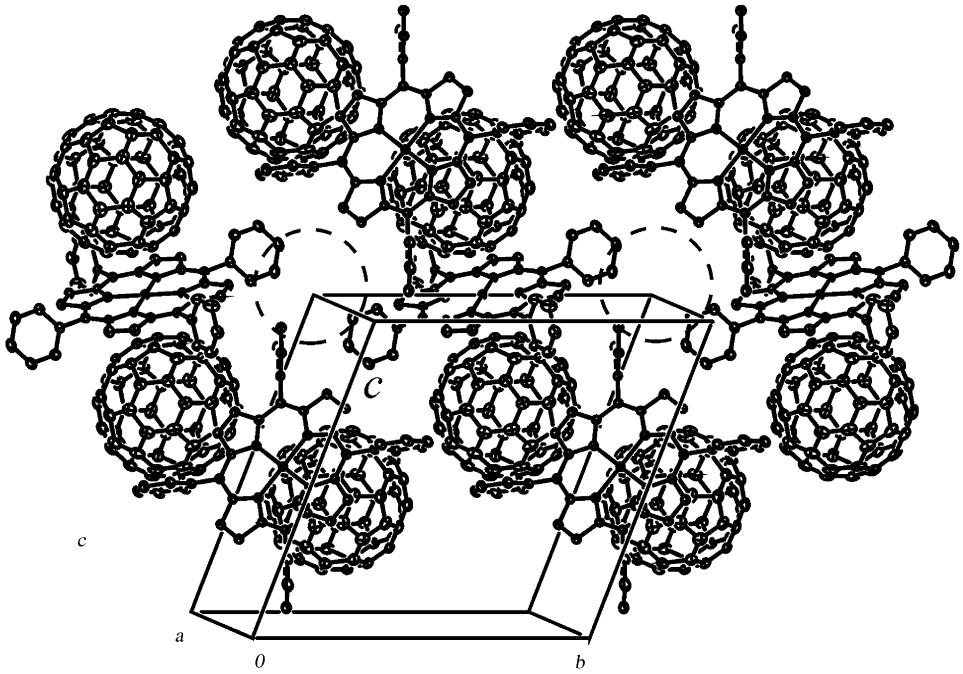

Figure 4. The fragment of crystal structure of $[Co^{II}(tpp)](C_{60})\cdot 2.5\,C_6H_4Cl_2$ (**4**) (the view on the *bc* plane). The channels shown by the dashed circles are occupied by the $C_6H_4Cl_2$ molecules (not depicted in figure). Only the major orientation of the C_{60} molecules is shown.

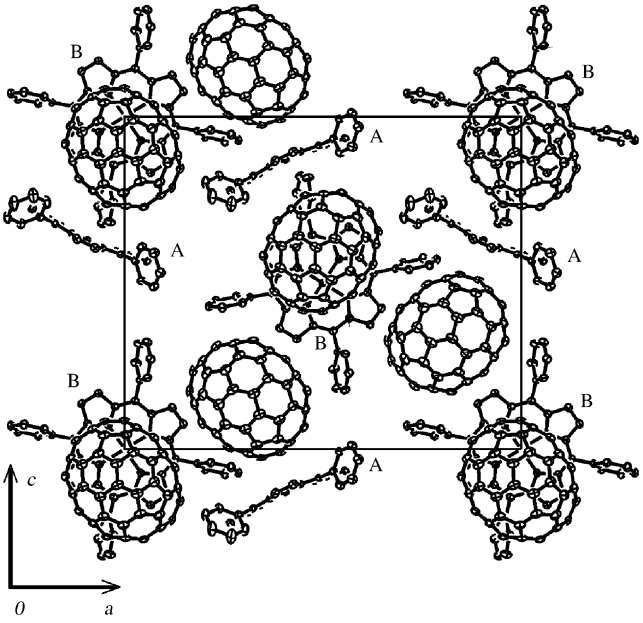

Figure 5. Fragment of the crystal structure of $[Co^{II}(tpp)](C_{70})\cdot 1.3\,CHCl_3\cdot 0.2\,C_6H_6$ (**6**). The view along the C_{70} layers is shown.

remain almost unchanged in **1**, **3**, **4**, and **6** as compared with the parent porphyrin,[34] whereas the N···Co bonds are noticeably elongated. The cobalt atom in **1** and **3** coordinates to fullerenes and TPP in a flattened square-pyramidal manner, deviating by 0.096(3) and 0.091(3) Å (**1**) and 0.113(1) Å (**3**) from the mean plane of the porphyrin macrocycle toward fullerene. The deviations of the cobalt atom in **1** and **3** are comparable with that in $[M^{II}(tpp)(py)]_2[Fe^{II}(Cp)_2]\cdot(C_{60})\cdot C_6H_5Me$ (the deviation of the cobalt atom toward pyridine is 0.190 Å[26e]).

Porphyrin macrocycles in the complexes with fullerenes have nearly planar geometry excepting $Co^{II}(tpp)$ "**A**" molecule in **6**, which has a noticeable saddle-like deviation (Table 2). The $[Co^{II}(tpp)]$ units in **9** are also bent in a saddle-like manner as in the parent $Co^{II}(tpp)$.[33]

IR spectra: Neutral C_{60} has four IR-active absorption bands at 527, 577, 1181, and 1429 cm^{-1} ($F_{1u}(1-4)$ modes, respectively). The frequency of the $F_{1u}(4)$ mode is sensitive to charge transfer to the C_{60} molecule.[35] This mode has two components (1408 and 1398 cm^{-1}) in **1**, which are noticeably shifted by 21–31 cm^{-1} to smaller wave numbers relative to parent C_{60}, and becomes close to that in C_{60} ionic salts with the 1^- charge on the C_{60} molecule: 1390–1394 cm^{-1} in $(Ph_4X^+)_2\cdot(C_{60}^{\bullet-})\cdot Y^-$ (X = P, As; Y = Cl, I),[36] and $Rb^+[C_{60}]^{\bullet-}$ at 1392 cm^{-1}.[35] The essential increase in the integral intensity of the $F_{1u}(2)$ mode relative to that of $F_{1u}(1)$ is also characteristic of $C_{60}^{\bullet-}$.[35] The splitting of the $F_{1u}(4)$ mode into two bands can be caused by the presence of two differently charged fullerene molecules or the lowering of C_{60} symmetry in the σ-bonded $[Co^{II}(tpp)(C_{60})]$ units. Several new weak bands at 548, 1196, 1204, 1232, 1262, and 1309 cm^{-1} can be attributed to the "silent" symmetry-forbidden modes of C_{60}, which appear as a result of symmetry breaking[37] in C_{60} at the formation of the σ-bonded $[Co^{II}(tpp)(C_{60})]$ units.

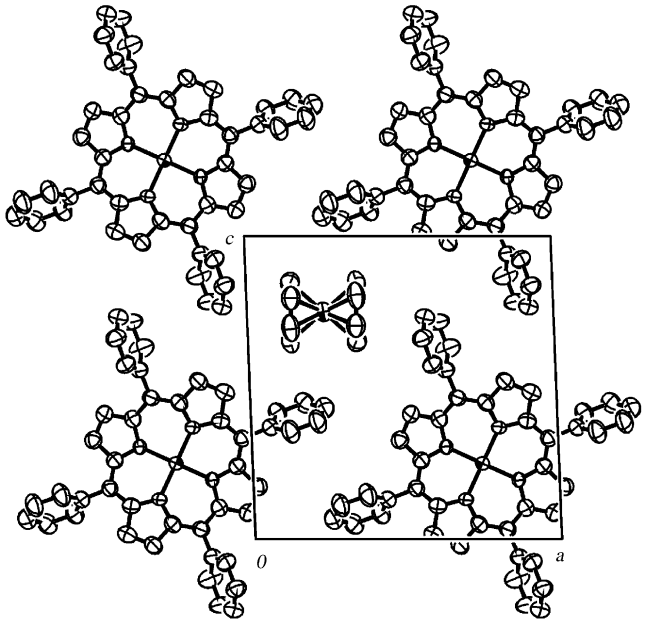

Figure 6. Crystal packing of $[Cr^0(C_6H_6)_2][Co^{II}(tpp)]$ (**9**).

Table 2. Geometry of the TPP macrocycle and selected bond lengths and angles in Co^{II}(tpp) molecules along with the shortest metal–fullerene contacts in **1, 3, 4**, and **6** and related compounds. For the notation for chemically equivalent bonds and bond angles see formula; for the **A** and **B** moieties see Figure 1a (**1**), b (**3**), c (**4**), and d (**6**).

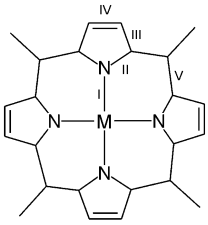

Compound	**1**	**3**	**4**	**6**	**9**	[{(Co(tpp)(py)]$_2$-[Fe(Cp)$_2$(C$_{60}$)] · C$_6$H$_5$Me[26e]	[Co(tpp)][34]
porphyrin	A/B		A/B	A/B			
geometry	planar	planar	planar	saddle/planar	saddle	planar	saddle
rms[a] [Å]	0.035/0.048	0.085	0.016/0.014	0.193/0.035	0.436	–	–
Δ [M][b] [Å]	0.096(3)/0.091(3)	0.113(1)	0.0/0.0	0.009(1)/0.0	–	0.190	–
bond lengths [Å][c]							
I	1.974(3)/1.974(2)	1.980(11)	1.979(9)/1.982(2)	1.976(5)/1.980(10)	1.923(2)	1.985(1)	1.948(1)
II	1.386(3)/1.388(8)	1.379(5)	1.381(3)/1.381(3)	1.379(4)/1.382(2)	1.402(5)	1.375(1)	1.378(1)
III	1.430(8)/1.440(8)	1.441(6)	1.440(4)/1.438(4)	1.432(4)/1.433(3)	1.435(7)	1.438(1)	1.441(1)
IV	1.353(16)/1.357(16)	1.347(5)	1.349(1)/1.352(1)	1.340(3)/1.346(4)	1.350(6)	1.348(2)	1.361(1)
V	1.387(6)/1.394(5)	1.387(5)		1.389(5)/1.391(2)	1.388(4)/1.389(4)	1.386(7)	1.391(1)
1.390(1)							
bond angles [°][c]							
I–II	127.7(2)/127.9(6)	127.5(2)	127.6(2)/127.5(4)	127.4(4)/127.6(4)	127.6(6)	127.4(1)	127.4(2)
II–II	104.3(5)/104.2(4)	104.9(5)	104.9(2)/105.0(1)	105.1(6)/104.8(2)	104.3(3)	104.9(1)	105.1(2)
II–III	110.8(6)/111.1(5)	110.6(4)	110.6(2)/110.5(2)	110.2(3)/110.5(2)	110.2(3)	110.7(1)	110.8(2)
III–IV	107.0(4)/106.8(6)	106.9(5)	107.0(2)/107.0(2)	107.3(2)/107.1(1)	107.5(6)	106.8(1)	106.6(2)
II–V	125.7(3)/125.7(1)	125.7(3)	126.0(2)/126.1(2)	125.8(7)/125.8(3)	124.0(6)	125.9(1)	125.6(2)
V–V	122.9(4)/122.8(6)	123.4(1)	122.9(2)/122.9(3)	123.5(5)/123.2(2)	122.3(3)	123.0(2)	121.9(2)
Co···C(fullerene) lengths [Å]	2.294(10)/2.319(9)	2.283(3) – C$_{60}$(**A**), 2.790(3) and 2.927(3) – C$_{60}$(**B**)	2.691(3) and 2.796(3)/2.690(3)	2.701(3), 2.739(3) and 2.899(3)/2.751(3)	–	2.82 – 3.49	–

[a] Root-mean-square (rms) deviations of atoms from the mean plane in the porphyrin macrocycle. [b] Deviation of the cobalt atom from the mean plane of the porphyrin macrocycle (△). [c] In brackets—standard deviation of the mean value over the porphyrin macrocycle.

The most intense IR-active bands of neutral C_{70} at 535, 794, and 1429 cm^{-1} are shifted in **2** to 530, 800, and 1391 cm^{-1}. The shift of the band of C_{70} from 1429 cm^{-1} (neutral) to 1391 cm^{-1} (**2**) is similar to that of the $F_{1u}(4)$ mode of C_{60} in its ionic salts[35, 36] and **1**, and indicates the formation of $C_{70}^{\bullet-}$. Numerous new bands attributed to symmetry breaking in C_{70} appear at 495, 546, 844, 944, 1110, 1154, 1204, 1244, 1259, 1280, and 1315 cm^{-1}.

Neutral $C_{60}(CN)_2$ has more than 17 bands, with the most intense ones at 766, 1430, and 2241 cm^{-1} (the C≡N stretching mode). These bands are noticeably shifted in **3** to 738, 1391, and 2230 cm^{-1}. The close position of the C≡N stretching mode was observed in ionic $[Co^{III}(Cp)_2]^+[C_{60}(CN)_2]^{\bullet-} \cdot CS_2$ (2233 cm^{-1}).[38]

Two IR bands are sensitive to charge transfer in $Cr^0(C_6H_6)_2$ and are shifted from 459 to 415 cm^{-1} and from 490 to 466 cm^{-1} at the transition from the neutral to the radical cation state in $[Cr^I(C_6H_6)_2]^{\bullet+} \cdot I^-$.[34] The position of these bands at 418 and 460 cm^{-1} in the spectra of **1**–**3** indicates the radical cation state of $[Cr^I(C_6H_6)_2]^{\bullet+}$.

The IR spectra of **4**–**8** are a superposition of the spectra of the starting components in their neutral states. The bands of fullerenes retain both the positions (within ±2 cm^{-1}) and the initial ratio of the intensities relative to parent molecules. The position of the IR bands of Co^{II}(tpp) in the spectra of **4**–**8** is shifted by 6 cm^{-1} relative to parent Co^{II}(tpp); this indicates small changes in its initial geometry in the complexes with fullerenes.

The IR spectrum of **9** consists of the bands of Co^{II}(tpp) (shifted by up to 10 cm^{-1} relative to parent Co^{II}(tpp)) and those of $Cr^0(C_6H_6)_2$.

UV/vis/NIR spectra: The spectra of solid **1**–**3** exhibit an essentially ionic ground state (Table 3). The bands of fullerenes and Co^{II}(tpp) are shifted in the complexes by 300–400 cm^{-1} to higher and lower energies, respectively, relative to the parent compounds.

New bands are also observed in the NIR spectra of **1**–**3**. The bands B at 9.3×10^3 (**1**), 8.1×10^3 (**2**), and 9.5×10^3 cm^{-1} (**3**) are attributed to (fullerene)$^{\bullet-}$ (Figure 7a–c). These bands have positions close to those in the solution spectra of $C_{60}^{\bullet-}$ and $C_{60}(CN)_2^{\bullet-}$: $9.2-9.4 \times 10^3$,[4] and 9.8×10^3 cm^{-1},[38] respectively. The band of $C_{70}^{\bullet-}$ in **2** is shifted to higher energy relative to that of $C_{70}^{\bullet-}$ in solution ($7.2-7.4 \times 10^3$ cm^{-1}[4]). The intense bands A at 7.8×10^3 (**1**), 10.9×10^3 (**2**), and 8.3×10^3 cm^{-1} (**3**) are ascribed either to transitions in the σ-bonded [Co^{II}(tpp)(fullerene)] units or charge transfer between fullerene anions. Relatively weak bands C in the visible range

Table 3. UV/vis/NIR spectra of the starting compounds and **1**–**9**.

Compounds	The bands of fullerenes and their anions, $\times 10^3$ cm^{-1}		Co^{II}(tpp) $\times 10^3$ cm^{-1}		CT bands $\times 10^3$ cm^{-1}		
	UV/vis range	NIR range	Soret band	Q-band	**A**	**C**	**D**
C_{60}	37.6, 29.1, 23.0						
C_{70}	–, 29.1, 25.8, 20.0						
$C_{60}(CN)_2$	38.2, 30.5, 23.8						
Co^{II}(tpp)			23.8	18.7			
1	37.9, 29.1	9.3	23.4	18.8	7.8	12.8	
2	–, 29.9	8.1	23.5	18.7	10.9	15.4	
3	38.3, 30.7	9.5	23.4	18.8	8.3		
4	38.1, 29.7		23.3	18.6			13.5
5	37.9, 29.6		23.4	18.7			13.5
6	39.5, 29.7		23.3	18.7			13.2
7	–, 29.7		23.4	18.8			13.3
8	38.2, 30.8		23.3	18.7			12.3
9[a]			23.8	18.8			

[a] The spectrum of **9** also contains the bands of Co^{II}(tpp) at 38.0×10^3 and of $Cr^0(C_6H_6)_2$ at 30.9×10^3 cm^{-1}.

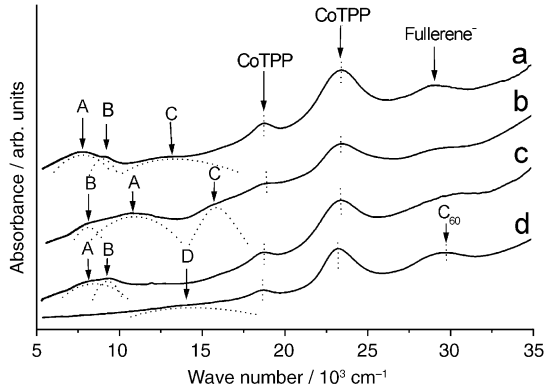

Figure 7. The UV/vis/NIR spectra of: a) $[\{Cr^I(C_6H_6)_2\}]_{1.7}[\{Co^{II}(tpp)(C_{60})\}_2]\cdot 3.3\,C_6H_4Cl_2$ (**1**); b) $[\{Cr^I(C_6H_6)_2\}_2][Co^{II}(tpp)(C_{70})](C_{70})\cdot 2\,C_6H_4Cl_2$ (**2**); c) $[\{Cr^I(C_6H_6)_2\}_2][Co^{II}(tpp)\{C_{60}(CN)_2\}][C_{60}(CN)_2]\cdot 3\,C_6H_4Cl_2$ (**3**); d) $[Co^{II}(tpp)](C_{60})\cdot 2.5\,C_6H_4Cl_2$ (**4**). The arrows and dashed curves show the positions of the bands in the vis–NIR range. The assignment is given in the text.

(Figure 7a and b) can be ascribed to charge transfer between (fullerene$^-$) and $Cr^I(C_6H_6)_2^{\bullet+}$.

The ground state of solid **4**–**8** is a neutral CT one because the UV/vis/NIR spectra do not exhibit the characteristic bands of (fullerene)$^{\bullet-}$ (Figure 7d). The bands of Co^{II}(tpp) and fullerenes are shifted in **4**–**8** by up to 880 cm^{-1} ($\sim$0.07 eV) to the red and blue sides, respectively, relative to parent compounds (Table 3). Weak and broad bands with maxima at $13-14 \times 10^3$ (**4**–**7**) and 12.3×10^3 cm^{-1} (**8**) are attributed to intermolecular charge transfer from Co^{II}(tpp) to fullerenes (band D). The energy of CT for the $C_{60}(CN)_2$ complex (**8**) is $\sim$0.1 eV lower than those for the C_{60} and C_{70} complexes (**4**–**7**); this indicates stronger acceptor properties of $C_{60}(CN)_2$.

The spectrum of **9** reveals the bands ascribed to Co^{II}(tpp) (38.0, 23.8, and 18.8 $\times 10^3$ cm^{-1}) and $Cr^0(C_6H_6)_2$ (30.9×10^3 cm^{-1}).

EPR spectra: The EPR parameters of the complexes are listed in Table 4. Only one Lorenzian signal is observed in the spectra of **1** and **3** (Figure 8a and c) at room temperature

Table 4. EPR parameters (g factor and line half width (ΔH)) for the obtained compounds at RT (290 K) and 4 K.

Compound	Attribution of the signal		RT		4 K	
			g factor	ΔH [mT]	g factor	ΔH [mT]
1	$[Cr^I(C_6H_6)_2]^{\bullet+}$		1.9861	11.0	1.9863	2.4
2	$[Cr^I(C_6H_6)_2]^{\bullet+}$	g_2	1.9856	5.3	1.9924	6.7
	$C_{70}^{\bullet-}$	g_1	2.0238	14.0	2.0606	21.0
3	$[Cr^I(C_6H_6)_2]^{\bullet+}$	g_2			1.9821	1.5
	$[Cr^I(C_6H_6)_2]^{\bullet+}$ + $C_{60}(CN)_2^{\bullet-}$[a]	g_1	1.9912	10.3	1.9934	2.1
4	$[Co^{II}(tpp)]$, $\perp$		2.5705	29.4	2.4731	24.6
	$[Co^{II}(tpp)]$, $\parallel$		2.2872	44.6	2.3966	36.8
6	$[Co^{II}(tpp)]$, $\perp$		2.6397	26.8	2.4654	22.4
	$[Co^{II}(tpp)]$, $\parallel$		2.4226	43.0	2.3241	35.0
8	$[Co^{II}(tpp)]$, $\perp$		2.5110	15.2	2.4605	16.6
	$[Co^{II}(tpp)]$, $\parallel$		2.3240	31.0	2.3046	27.0
9	$[Co^{II}(tpp)]$			absent	2.52	286.0
	$[Cr^I(C_6H_6)_2]^{\bullet+}$, $\perp$				1.9899	2.1
	$[Cr^I(C_6H_6)_2]^{\bullet+}$, $\parallel$				1.9828	1.1

[a] The signal is characteristic of strong exchange coupling between $Cr^I(C_6H_6)_2^{\bullet+}$ and corresponding fullerene radical anions.

(RT = 290 K). The g factor of the EPR signal of **1** is close to that in ionic $[Cr^I(C_6H_6)_2]^{\bullet+}[C_{60}]^{\bullet-}$ ($g = 1.9860$)[39] or $[Cr^I(C_6H_6)_2]^{\bullet+}$ in rigid solution ($g = 1.9860$).[40]

Figure 9 shows the temperature dependency of the g factor and the line half width (ΔH) of the EPR signal of **3**. The signal becomes narrower with decreasing temperature down to 180 K, and then remains almost constant (1.5–2.1 mT) in the 4–180 K range. At $T < 180$ K, the signal becomes asymmetric and is simulated by the two Lorenzian components with $g_1 = 1.996$ ($\Delta H = 1.6$ mT) and $g_2 = 1.988$ ($\Delta H = 1.9$ mT) at 150 K (Figure 8c). After the splitting, the g factors of the two components are shifted to lower values with decreasing temperature. The temperature dependency of the g factor and ΔH of the EPR signal of **1** is similar to that of **3** (for the component with g_2).

The EPR signal of **2** is asymmetric at RT with the two components centered at $g_1 = 2.0238$ ($\Delta H = 14$ mT) and $g_2 = 1.9856$ ($\Delta H = 5.3$ mT) (Figure 8b). Both signals become broad with decreasing temperature down to 4 K ($\Delta H = 21$ and 6.7 mT, respectively) and are shifted to higher g factors.

The EPR spectra of **4**, **6**, and **8** have intense asymmetric signals with $g_\parallel = 2.28-2.42$ ($\Delta H = 31-45$ mT) and $g_\perp = 2.51-2.64$ ($\Delta H = 15-30$ mT) depending on fullerene (Figure 8d). The values of $g_\parallel$ and $g_\perp$ become closer to each other with decreasing temperature down to 4 K and are equal to 2.3–2.4 and 2.46–2.47, respectively.

Complex **9** is EPR silent at RT and shows a very broad signal at 4 K (Table 4) attributed to Co^{II}(tpp). The asymmetric signal characteristic of $[Cr^I(C_6H_6)_2]^{\bullet+}$[40] is also observed at 4 K. However, its integral intensity is only 0.1 % from that of Co^{II}(tpp).

Magnetic properties: The data of SQUID magnetic susceptibility measurements (1.9–300 K) of **1**–**3** and **8** are presented in Table 5. The experimental data were corrected by the sample-holder contribution and core-diamagnetic contributions. Magnetic susceptibilities of **1**–**3**, and **8** follow the

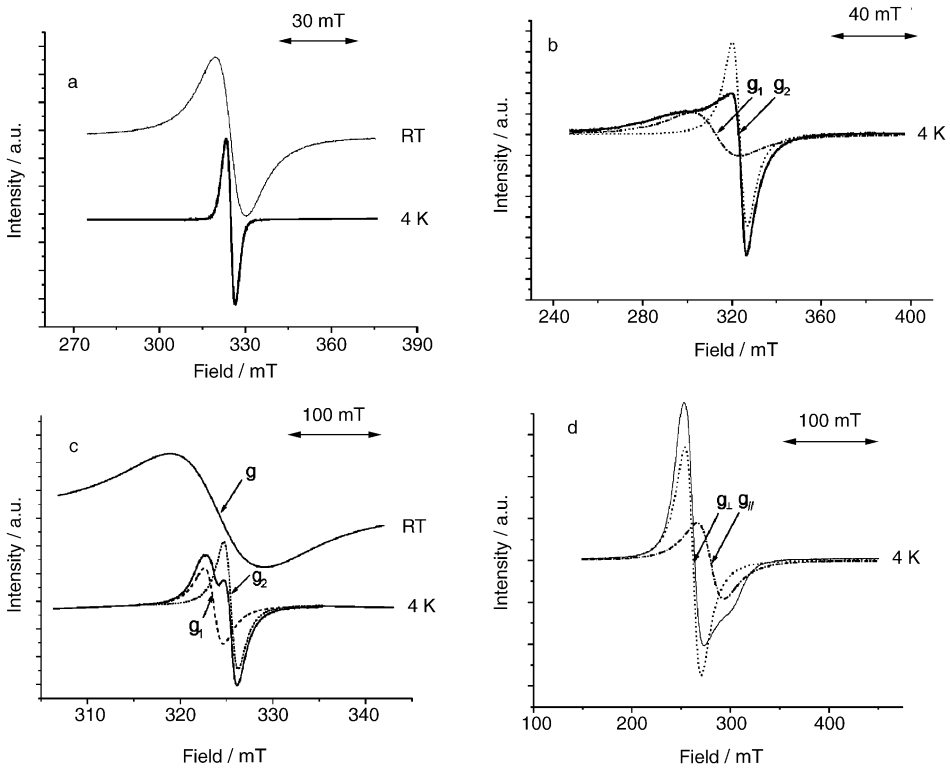

Figure 8. EPR spectra of: a) $[\{Cr^{I}(C_6H_6)_2\}_{1.7}][\{Co^{II}(tpp)(C_{60})\}_2]\cdot 3.3\,C_6H_4Cl_2$ (**1**) at RT (285 K) and 4 K; b) $[\{Cr^{I}(C_6H_6)_2\}_2][Co^{II}(tpp)(C_{70})](C_{70})\cdot 2\,C_6H_4Cl_2$ (**2**) at 4 K; c) $[\{Cr^{I}(C_6H_6)_2\}_2][Co^{II}(tpp)\{C_{60}(CN)_2\}]$-$[C_{60}(CN)_2]\cdot 3\,C_6H_4Cl_2$ (**3**) at RT and 4 K; d) $[Co^{II}(tpp)](C_{60})\cdot 2.5\,C_6H_4Cl_2$ (**4**) at 4 K. Dotted and dashed lines show the simulation of the EPR spectrum by the two Lorenzian lines.

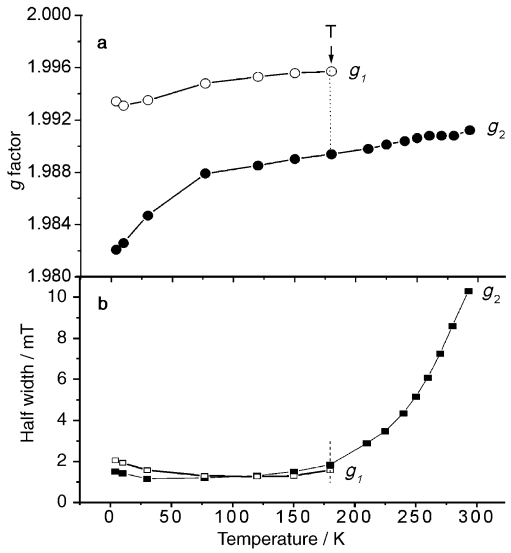

Figure 9. Temperature dependency of EPR parameters a) g factors and b) the line half width (ΔH) of the EPR signal from $[\{Cr^{I}(C_6H_6)_2\}_2]$-$[Co^{II}(tpp)\{C_{60}(CN)_2\}][C_{60}(CN)_2]\cdot 3\,C_6H_4Cl_2$ (**3**) in the 4–300 K range. Open and closed symbols correspond to the g_1 and g_2 components, respectively. "T" denotes the temperature of the splitting of the EPR signal into two components.

Curie–Weiss law. The Weiss constants (θ) determined from the plots based on the equation $1/\chi_M = C(T-\theta)$ are also shown in Table 5.

The number of spins per formula unit was calculated from the magnetic moment of the complexes at 300 K (Table 5).

The temperature dependencies of μ_{eff} for **1**–**3** and **8** are qualitatively similar. Figure 10 shows the results for **3** as an example. A small decrease of μ_{eff} is observed with the temperature decrease down to 200 K, then μ_{eff} remains unchanged down to 50 K. At 2–50 K, the magnetic moment decreases in **1**–**3** and **8** due to antiferromagnetic interactions of spins.

Conductivity: The compounds are semiconductors with RT (290 K) conductivity: 4×10^{-5} for **1**, 4×10^{-6} for **2**, and $2\times10^{-3}\,S\,cm^{-1}$ for **3**. The complexes **4**–**8** are dielectric ($\sigma < 10^{-7}\,S\,cm^{-1}$).

Discussion

The complexes of Co^{II}(tpp) with fullerene radical anions: H_2(tpp), Co^{II}(tpp), Cu^{II}(tpp), and Zn^{II}(tpp) form various complexes with neutral fullerenes.[22, 23, 26] However, only Co^{II}(tpp) forms ionic multicomponent complexes **1**–**3** with fullerene radical anions.

According to the X-ray structure analysis, $[\{Cr^{I}(C_6H_6)_2\}_{1.7}]$-$[\{Co^{II}(tpp)(C_{60})\}_2]\cdot 3.3\,C_6H_4Cl_2$ (**1**) contains a nonstoichiometric amount of $Cr^{I}(C_6H_6)_2$ relative to C_{60} ($\sim$1.7:2). Since

Table 5. Data of magnetic measurements.

Compound	θ [K]	T range [K]	Obs[b]	μ_{eff} at 300 K [μ_B] Calcd	μ_{eff} calcd[a]
1	−0.83	10–200	2.40	2.26 (1.7 spins with $S=½$)	4.14
2	+3.76	20–230	2.98	3.00 (3 spins with $S=½$)	3.87
3	−2.43	20–200	2.91	3.00 (3 spins with $S=½$)	3.87
8	+2.87	25–200	1.83	1.73 (1 spin with $S=½$)	1.73

[a] From the composition of the complex ($S=½$ for Co^{II}(tpp), $Cr^{I}(C_6H_6)_2^{\cdot+}$ and (fullerenes)$^{\cdot-}$). [b] From SQUID measurements

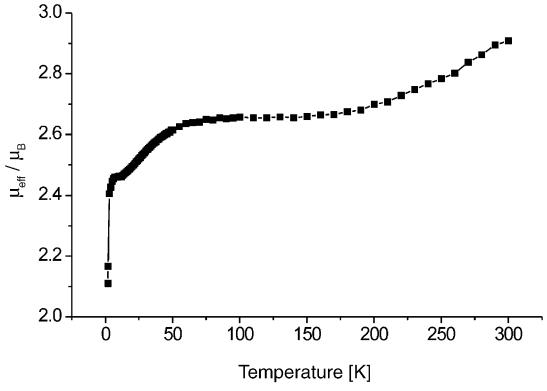

Figure 10. Temperature dependency of the effective magnetic moment of $[\{Cr^{I}(C_6H_6)_2\}_2][Co^{II}(tpp)\{C_{60}(CN)_2\}][C_{60}(CN)_2]\cdot 3\,C_6H_4Cl_2$ (**3**) in the 1.9–300 K range.

$Cr^{I}(C_6H_6)_2$ forms radical cations in **1**, the formal charge on the two C_{60} molecules is 1.7−. Thus, two differently charged fullerene molecules can be present in the complex. Actually, two different fullerenes were observed in the crystal structure, and two bands for the $F_{1u}(4)$ mode were pronounced in the IR spectrum. A 1:1 molar ratio of $Cr^{I}(C_6H_6)_2^{\bullet+}$ to C_{70} or $C_{60}(CN)_2$ in **2** and **3** gives the 1− formal charge on fullerene molecules that is consistent with the optical data.

The number of spins estimated from the magnetic susceptibility of **1**–**3** at 300 K (Table 5) is essentially smaller than that expected from the composition of these complexes (Co^{II}(tpp), $Cr^{I}(C_6H_6)_2^{\bullet+}$, and (fullerenes)$^{\bullet-}$ formally have $S=$ ½ each). The magnetic moment of **1** (2.4 μ_B per formula unit) is close to an uncorrelated 1.7 $S=$ ½ system (μ_{eff} of 2.26 μ_B). Since the EPR signal of **1** is characteristic of $Cr^{I}(C_6H_6)_2^{\bullet+}$,[40] it is deduced that these spins are localized mainly on $Cr^{I}(C_6H_6)_2^{\bullet+}$.

The magnetic susceptibilities of **2** and **3** at 300 K (2.91–2.98 μ_B) are defined by three noninteracting spins per formula unit (the spin-only value is 3.00 μ_B). The EPR signal of **2** has two components at RT, whereas that of **3** is split into two components below 180 K (Figures *c* and 9, Table 4). The two components (g_1 and g_2) can be attributed to $Cr^{I}(C_6H_6)_2^{\bullet+}$ (g_2) and $C_{70}^{\bullet-}$ (g_1) in **2** and to $Cr^{I}(C_6H_6)_2^{\bullet+}$ (g_2) and the resonating signal (g_1) between $C_{60}(CN)_2^{\bullet-}$ and $Cr^{I}(C_6H_6)_2^{\bullet+}$ in **3**. The resonating signal is characteristic of a strong exchange coupling and has a mean g factor between those of $Cr^{I}(C_6H_6)_2^{\bullet+}$ ($g=1.9860$[40]) and $C_{60}(CN)_2^{\bullet-}$ ($g=1.9998$[38]). The EPR signal of $C_{70}^{\bullet-}$ has a higher g factor value ($g=$ 2.0238) in **2** than that in $(Ph_4P^+)_2(C_{70}^{\bullet-})\cdot I^-$ ($g_{av}=2.0047$[42]). Therefore, an exchange coupling between $C_{70}^{\bullet-}$ and Co^{II}(tpp) is possible. Additional structural data allow the nature of this coupling to be elucidated. In accordance with the EPR data, three spins per formula unit are basically localized in **2** and **3** on $Cr^{I}(C_6H_6)_2^{\bullet+}$ (two spins with $S=$ ½) and the nonbonding fullerene$^{\bullet-}$ (one spin with $S=$ ½). Consequently, the σ-bonded [Co^{II}(tpp)(fullerene)]$^-$ anions are deduced to be diamagnetic in **1**–**3**.

X-ray-diffraction analysis shows that both C_{60} molecules are σ-bound with the Co^{II}(tpp) units in **1**, whereas only one of two fullerene anions has such coordination in **3**. Accordingly, the ionic formulas of **1** and **3** are: $[\{Cr^{I}(C_6H_6)_2\}^{\bullet+}]_{1.7}[\{Co^{II}(tpp)(C_{60})\}_2]^{1.7-}\cdot 3.3\,C_6H_4Cl_2$ (**1**), and $[\{Cr^{I}(C_6H_6)_2\}^{\bullet+}]_2[Co^{II}(tpp)\{C_{60}(CN)_2\}^-][C_{60}(CN)_2^{\bullet-}]\cdot 3\,C_6H_4Cl_2$ (**3**). Complexes **2** and **3** have similar composition and a close value of the magnetic moment. By analogy with **3**, the ionic formula of **2** might be given as $[\{Cr^{I}(C_6H_6)_2\}^{\bullet+}]_2[Co^{II}(tpp)(C_{70})^-](C_{70})^{\bullet-}\cdot 2\,C_6H_4Cl_2$.

The Co–C(fullerene) bond lengths for σ bonding vary over the 2.28–2.32 Å range. These bond lengths are longer than those in the strong covalent Co–C bond in alkylcobaltoamines (1.99–2.03 Å)[43] but are essentially shorter than the M$\cdots$C(fullerene) bond lengths (in the 2.61–3.00 Å range) in the complexes of neutral fullerenes with metal-containing tetraphenyl- and octaethylporphyrins.[22, 23, 25–28] The UV/vis/NIR spectra of **1**–**3** exhibit a noticeable redistribution of electronic levels in both Co^{II}(tpp) and fullerene anions relative to the starting ones. Thus, the σ bonding results in noticeable changes in the electronic structure of the starting components.

The Co(tpp) complexes with neutral fullerenes: According to the IR and UV/vis/NIR spectra, **4**–**8** have a neutral ground state. However, a noticeable interaction of the π system of fullerenes with the d–π system of Co(tpp) is observed. The EPR spectra of **4**, **6**, and **8** and magnetic susceptibility measurements for **8** reveal only one unpaired electron per formula unit localized on Co^{II}(tpp) with an $S=$ ½ ground state. The EPR spectra of the complexes are essentially different from that of parent Co^{II}(tpp) ($g_\perp=3.322$, $g_\parallel=1.798$)[44] due to the changes in the hyperfine interaction parameters, which are the most sensitive to the local environment of the metal center. The EPR spectra of **4**, **6**, and **8** are similar to those of the Co^{II}(tpp)$\cdot$A compounds in which A is a strongly coordinated CO, $P(OCH_3)_3$, or py ligand. These compounds have asymmetric spectra with $g_\parallel=2.017-2.027$ and $g_\perp=2.17$-2.32 in solution.[41] That the $g_\parallel$ value in Co^{II}(tpp)$\cdot$A is larger than the theoretically calculated $g=$ 2.002 expected for a pure $(d_{z^2})^1$ ground state is attributed to the elevation of the d_{z^2} level and the contribution of $d_{x^2-y^2}$ to the ground state due to orbital mixing.[41, 45] A similar increase in the $g_\parallel$-factor values relative to 2.002 is also observed in the Co^{II}(tpp)–fullerene complexes.

Shortened contacts are formed in **4** and **6** between the cobalt or nitrogen atoms of Co^{II}(tpp) and the C_{60} or C_{70} carbons (d–π and π–π interactions, respectively). The Co$\cdots$C(C_{60} or C_{70}) contacts of 2.69–2.75 Å in **4** and **6** are close to those in various neutral C_{60} and C_{70} complexes with cobalt-containing tetraaryl- and octaethylporphyrins: $[Co^{II}(tbp)](C_{60})$: 2.61 Å,[26d] $[Co^{II}(tmpp)](C_{60})\cdot C_6H_5Me$: 2.64 Å,[26e] $[Co^{II}(oep)]_2(C_{60})\cdot CHCl_3$: 2.74 Å,[25a] and $[Co^{II}(oep)](C_{70})\cdot C_6H_6\cdot CHCl_3$: 2.80 Å.[25a] These contacts are shorter than nonbonded van der Waals contacts (3.1–3.3 Å) but are significantly longer than strong η^2-coordination (2.1–2.2 Å) and can be described as a secondary bonding.

The red shift of the Soret and Q-bands of Co^{II}(tpp) in the UV/vis/NIR spectra of **4**–**8** relative to those of the parent Co^{II}(tpp) is similar to the shift of these bands in **1**–**3**, and reported for the [Co^{II}(tpp)(A)] compounds.[41] Thus, these shifts are common for the coordination of different ligands (including fullerenes) to Co^{II}(tpp).

The complex $[Cr^0(C_6H_6)_2][Co^{II}(tpp)]$ (9): is afforded as a result of crystallization of Co^{II}(tpp) in toluene in the presence of $[Cr^0(C_6H_6)_2]$. The $[Cr^0(C_6H_6)_2]$ and [Co^{II}(tpp)] units interact weakly through π–π interactions between the C_6H_6 groups of $[Cr^0(C_6H_6)_2]$ and the phenyl constituents of [Co^{II}(tpp)] According to the UV/vis/NIR and EPR spectra, **9** has a neutral ground state.

Bonding model of Co^{II}(tpp)]with neutral fullerenes and their radical anions: The [Co^{II}(tpp)(fullerene)$^{n-}$] ($n=0$, 1) complexes have some similarities with the [Co(tpp)(A)] compounds, in which A is a diatomic ligand CO or NO.[46] The model qualitatively describing the interaction between the Co^{II}(tpp) and A–B ligands with a bent Co$\cdots$A–B fragment can be used to describe the Co^{II}(tpp)–fullerene interaction. In this model C_{60} (π^{*0}), and $C_{60}^{\bullet-}$ (π^{*1}) have the same number of electrons on the π^* level as CO (π^{*0}), and NO (π^{*1}).

The interaction of the d_{z^2} orbital of Co^{II}(tpp) (d^7) and C_{60} t_{1u} π^* orbital removes the triple degeneracy of the C_{60} π^* level to produce two molecular orbitals (MO), which are essentially C_{60} π^* orbitals, and a third orbital capable of σ bonding with the metal d_{z^2}. The generalized MO scheme for the interaction of Co^{II}(tpp) with $C_{60}^{\bullet-}$ is shown in Figure 11 (only Co d and C_{60} π^* orbitals are shown).

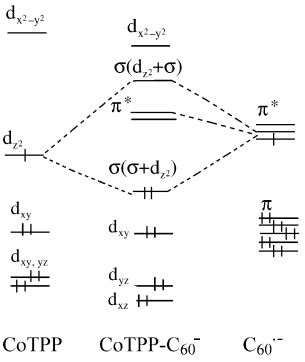

Figure 11. Schematic molecular-orbital diagram for the interaction of neutral C_{60} and its radical anion with Co^{II}(tpp) (C_{60} (π^{*0}), $C_{60}^{\bullet-}$ (π^{*1}), and Co^{II}(tpp) (d^7)).

For the interaction of Co^{II}(tpp) (d^7) with neutral C_{60} (π^{*0}), seven 3d-orbital electrons are placed in the MO scheme. Only one unpaired electron occupies the σ MO. The secondary bonding observed in **4** can be a result of the single occupancy of this σ MO. In this relation, **4** is similar to paramagnetic $[Co^{II}(tpp)(CO)]$.[41]

The electronic configuration for the interaction of Co^{II}(tpp) (d^7) with $C_{60}^{\bullet-}$ (π^{*1}) is obtained by placing one additional electron in the MO Scheme (Figure 11). The σ MO is occupied by two electrons. A two-electron covalent bond between Co and $C_{60}^{\bullet-}$ is formed. Given two-electron occupancy of the σ MO, the $[Co^{II}(tpp)(C_{60})^-]$ anion is diamagnetic. It should be noted that covalently bonded $[Co^{II}(tpp)(NO)]$ with a similar electronic configuration (Co^{II} (d^7), NO (π^{*1})) is also diamagnetic and EPR silent.[41]

Thus, the difference in the interaction of neutral and negatively charged fullerenes with Co^{II}(tpp) is associated with the presence of an additional electron at the π^* level of the fullerene anion, which can be involved in the σ bonding.

The electronic configuration (Co^{II}(tpp) (d^7), fullerene$^{\bullet-}$ (π^{*1})) for the interaction of Co^{II}(tpp) with $C_{60}(CN)_2^{\bullet-}$ or $C_{70}^{\bullet-}$ is similar to that for $C_{60}^{\bullet-}$. As a result, σ bonding is also observed in **2** and **3**, and the resulting $[Co^{II}(tpp)(fullerene)]^-$ anions are diamagnetic. However, the σ bonding of Co^{II}(tpp) to $C_{60}(CN)_2^{\bullet-}$ in **3** is only observed for one of the two fullerene anions. Similarly, in $[Fe^{II}(tpp)(NO)]\cdot NO$ only one of the two NO ligands coordinates to Fe^{II}(tpp).[45]

Conclusion

New fullerene complexes of Co^{II}(tpp) with ionic (**1**–**3**) and neutral (**4**–**8**) ground states have been obtained. The multicomponent approach has allowed us to study the interaction of Co^{II}(tpp) with negatively charged fullerenes C_{60}, C_{70}, and $C_{60}(CN)_2$ for the first time. This interaction is characterized by σ bonding between Co^{II}(tpp) and a carbon cage with essentially shortened Co···C contacts of 2.28–2.32 Å. Thus, it is shown that fullerene radical anions are able to be essentially more strongly bound to Co^{II}(tpp) than neutral fullerenes. The possibility for σ bonding is associated with the presence of an additional electron on the π^* level of fullerenes$^{\bullet-}$ that interacts with the d_{z^2} orbital of Co^{II}(tpp). This bonding results in the diamagnetism of the $[Co^{II}(tpp)(fullerene)]^-$ anions.

The complexes have cage structures with large cavities or channels accommodating $Cr^I(C_6H_6)_2^{\bullet+}$ and $C_6H_4Cl_2$. The size of the cavities allows the insertion of small donor molecules into the $[Co^{II}(tpp)(fullerene)]$ framework. The D_1 component affects the charged state of fullerenes and, consequently, conductive, magnetic, and optical properties of the complexes. The size of the D_1 component must be comparable to that of the solvent molecules to be incorporated in the complex, otherwise a multicomponent complex is not formed, as in the case of $Cr^{II}(Cp^*)_2$.

The characteristic features of the Co^{II}(tpp) complexes with neutral fullerenes (**4**–**8**) are secondary M···C(fullerene) bonding with the shortest Co···C contacts in the 2.69–2.75 Å range and minor changes in the electronic structure of the parent components. The absence of a noticeable degree of CT between Co^{II}(tpp) and fullerenes is associated with the relatively weak donor properties of Co^{II}(tpp) ($E_{1/2}^{+/0}$ of Co^{II}(tpp) is $+0.52$ V[46]).

Complexes **1**–**3** are paramagnets due to the magnetic dilution of the paramagnetic $[Cr^I(C_6H_6)_2]^{\bullet+}$ and the nonbonded (fullerene)$^{\bullet-}$ by the diamagnetic $[Co^{II}(tpp)(fullerene)]^-$ anions. The semiconductive behavior of **1**–**3**, with conductivities of 2×10^{-3}–4×10^{-6} S cm^{-1}, is characteristic of fullerene salts with bulky cations[5] and is attributed to the presence of diamagnetic $[Co(tpp)(fullerene)]^-$ anions, which gave rise to the localized nature of the (fullerene)$^{\bullet-}$ electrons rather than an itinerant one. At the same time, the photoactive properties of the compounds containing $[Co(tpp)(fullerene)]^-$ anions make them interesting as dyad analogues.[47] The multicomponent complexes can be developed by varying either the D_1 or D_2 components.

Experimental Section

Materials: Co^{II}(tpp) and $Cr^0(C_6H_6)_2$ were purchased from Aldrich and Strem Chemicals. C_{60} and C_{70} of 99.98 and 99.0% purity were used from MTR Ltd. $C_{60}(CN)_2$ was synthesized according to the literature procedure.[48] *o*-Dichlorobenzene was distilled over CaH_2 at reduced pressure under an argon atmosphere. Toluene, benzene, and hexane were distilled over Na/benzophenone under argon. Acetonitrile was distilled over CaH_2, P_2O_5, and K_2CO_3 under argon. $CHCl_3$ was passed through a column with activated alumina and distilled over CaH_2 under argon. The solvents were degassed before the synthesis of air-sensitive complexes **1**–**3** and **9** and were put into a glove box. All manipulations during the synthesis and isolation of the crystals of **1**–**3** and **9** were carried out in a MBraun 150B-G glove box with controlled atmosphere and a content of H_2O and O_2 of less than 1 ppm. The crystals were stored in the glove box and were sealed in 2 mm quartz tubes for EPR and SQUID measurements at 10^{-5} Torr. KBr pellets for IR and UV/vis/NIR measurements were also prepared in the glove box.

General: UV/vis/NIR spectra were measured on a Shimadzu-3100 spectrometer in the 240–2600 nm range. FTIR spectra were measured in KBr pellets with a Perkin–Elmer 1000 Series spectrometer (400–7800 cm^{-1}). A Quantum Design MPMS-XL SQUID magnetometer was used to measure static susceptibilities down to 1.9 K. A sample-holder contribution and core diamagnetic susceptibility (χ_0) were subtracted from the experimental data. The core diamagnetic contributions of -440, -141,[49] -83.2, -54.8, -59.2×10^{-6} emu mol^{-1} were used for Co^{II}(tpp), $Cr^0(C_6H_6)_2$, $C_6H_4Cl_2$, C_6H_6, and $CHCl_3$, respectively. The contribution of fullerenes to total susceptibility can be ignored since the diamagnetic and paramagnetic components cancel out.[50, 51] EPR spectra were recorded down to 4 K with a JEOL JES-TE 200 X-band ESR spectrometer equipped with a JEOL ES-CT470 cryostat. Conductivity was measured by a two-probe technique in the glove box on pressed pellets.

Synthesis: Crystals of **1**–**3** were obtained by diffusion. Co^{II}(tpp) (0.027 mmol), $Cr^0(C_6H_6)_2$ (0.054 mmol), and fullerenes (0.027 mmol) were dissolved at a 1:2:1 molar ratio in $C_6H_4Cl_2$ (20 mL), and the solution was filtered in a glass tube of 1.5 cm diameter and 40 mL volume. *n*-Hexane (20 mL) was layered over the $C_6H_4Cl_2$ solution, and after 1 month, the crystals of **1**–**3** were formed. The solvent was decanted, and the crystals of **1**–**3** were washed with *n*-hexane (50–70% yield).

The crystals of **5** and **8** were obtained by slow evaporation of C_6H_5Me (**5**) or $C_6H_6/CHCl_3$ (1:1) (**8**) solutions (30 mL) containing fullerene (0.027 mmol) and Co^{II}(tpp) (0.027 mmol) over 2 weeks. The crystals of **5** were washed with acetonitrile (70–90% yield). They were unstable in storage and decomposed over several weeks.

Crystals of **4** and **7** were obtained by diffusion of acetonitrile (20 mL) into a solution containing fullerene (0.027 mmol) and Co^{II}(tpp) (0.027 mmol) in $C_6H_4Cl_2$ (20 mL) over 1 month (40–60% yield). The crystals were unstable due to the loss of the solvent and were stored in $C_6H_4Cl_2$/acetonitrile (1:1).

Crystals of **6** were obtained by diffusion of a solution of C_{70} (0.027 mmol) in C_6H_6 (20 mL) into a solution of Co^{II}(tpp) (0.027 mmol) in $CHCl_3$ (10 mL) over 3 weeks. The solvent was decanted, and the crystals were washed with acetonitrile (40% yield).

Crystals of **9** were obtained by diffusion of a solution of $Cr^0(C_6H_6)_2$ (0.15 mmol) in acetonitrile (15 mL) into a solution of Co^{II}(tpp) (0.03 mmol) in C_6H_5Me (15 mL) (Co^{II}(tpp)/$Cr^0(C_6H_6)_2$ 1:5 molar ratio). The crystals were washed with acetonitrile to give a 30–60% yield.

The compositions of **1, 3, 4, 6, 9** and **2, 5, 7, 8** were determined by X-ray and elemental analyses, respectively. The composition of **1**–**3** was confirmed by microprobe analysis for a Co/Cr/Cl atomic ratio on a single crystal. The elemental analysis data and the shape of the crystals are presented in Table 1.

Crystal structure determination: The intensity data for the structural analysis were collected on a MAC Science DIP-2020 K oscillator-type X-ray imaging plate diffractometer with graphite monochromated $Mo_{K\alpha}$ radiation at 120 K by using an Oxford Cryostream cooling system or at room temperature. Raw data reduction to F^2 was carried out by using the DENZO program.[52] The structures were solved by direct method and refined by the full-matrix least-squares method against F^2 with SHELX-

Table 6. Crystal data for **1, 3, 4, 6** and **9**.

Compound	**1**	**3**	**4**	**6**	**9**
structural formula	$[\{Cr(C_6H_6)_2\}_{1.7}][\{Co(tpp)\}_2(C_{60})_2]\cdot3.3\,C_6H_4Cl_2$	$[\{Cr(C_6H_6)_2\}_4][\{Co(tpp)\}_2\{C_{60}(CN)_2\}_4]\cdot6\,C_6H_4Cl_2$	$[\{Co(tpp)\}_2(C_{60})_2]\cdot5\,C_6H_4Cl_2$	$[\{Co(tpp)\}_2(C_{70})_2]\cdot2.6\,CHCl_3\cdot0.4\,C_6H_6$	$[Cr(C_6H_6)_2][Co(tpp)]$
empirical formula	$C_{248.47}H_{89.89}Cl_{6.59}Co_2Cr_{1.73}N_8$	$C_{420}H_{128}Cl_{12}Co_2Cr_4N_{16}$	$C_{238}H_{76}Cl_{10}Co_2N_8$	$C_{233.08}H_{61.08}N_8Cl_{7.76}Co_2$	$C_{56}H_{40}CoCrN_4$
M_r [g mol^{-1}]	3627.87	6148.64	3519.43	3365.57	879.85
shape	black prism	black parallelepiped	black prism	black prism	black prism
size [mm^3]	$0.44\times0.18\times0.12$	$0.75\times0.25\times0.14$	$0.4\times0.4\times0.4$	$0.50\times0.4\times0.25$	$0.25\times0.20\times0.15$
crystal system	orthorhombic	triclinic	triclinic	orthorhombic	monoclinic
space group	$Pmn2_1$	$P\bar{1}$	$P\bar{1}$	*Pnma*	$P2/n$
a [Å]	15.5340(10)	13.967(1)	14.226(1)	26.240(3)	14.805(5)
b [Å]	19.1650(10)	15.928(1)	16.808(1)	23.869(3)	9.506(6)
c [Å]	27.0380(15)	30.332(1)	17.002(1)	22.006(3)	14.657(4)
α [°]	90	92.30(1)	68.974(1)	90	90
β [°]	90	100.89(1)	85.982(1)	90	92.21(2)
γ [°]	90	103.46(1)	77.651(1)	90	90
V [$Å^3$]	8049.5(8)	6419.3(6)	3706.8(5)	13783(3)	2061.2(1.5)
Z	2	1	1	4	2
ρ_{calcd} [g cm^{-3}]	1.497	1.591	1.577	1.622	1.418
radiation	graphite monochromated $Mo_{K\alpha}$, $\lambda=0.71073$				
μ [mm^{-1}]	0.497	0.494	0.479	0.468	0.712
absorption correction	none	none	none	semiempirical from equivalents	none
max./min. transmission	0.94/0.91	0.93/0.89	–	0.89/0.71	0.89/0.84
T [K]	120	120	120	120	300
max. 2θ [°]	55	55	55	50	53
reflns measured	42103	37757	23502	77463	14600
unique reflns	8885	22474	14555	12462	4464
R_{int}, R_σ	0.046, 0.034	0.026, 0.043	0.019, 0.033	0.053, 0.046	0.094,0.131
parameters	1238	2383	1552	1234	277
restraints	668	818	378	217	0
reflns $F_o>4\sigma F_o$	7628	17869	11895	8373	2453
R_1 [$F_o>4\sigma F_o$]	0.085	0.067	0.056	0.049	0.068
wR_2 (all data)[a]	0.243	0.188	0.142	0.128	0.160
a	0.149	0.104	0.054	0.075	0.036
b	15.2	9.0	4.8	0.0	0.0
G.O.F	1.041	1.024	1.034	1.012	0.999
restr. G.O.F	1.013	1.042	1.022	1.011	
largest diff. peak/hole	1.78/$-$0.55	1.60/$-$0.90	0.54/$-$0.54	1.16/$-$0.32	0.51/$-$0.30
rms	0.10	0.07	0.06	0.08	0.06

[a] $w=1/[\sigma^2(F_o^2)+(aP)^2+bP]$, $P=[\max(F_o^2,0)+2F_c^2]$

97.[53] The details of crystal structure analysis for the structures are given in the Table 6.

CCDC-193661–5 (compounds **9**, **1**, **4**, **6**, **3**, respectively) contain the supplementary crystallographic data for this paper. These data can be obtained free of charge via www.ccdc.cam.ac.uk/conts/retrieving.html (or from the Cambridge Crystallographic Data Centre, 12 Union Road, Cambridge CB2 1EZ, UK; fax: (+44) 1223-336033; or deposit@ccdc.cam.uk).

Acknowledgements

This work was supported by the COE Research on Elements Science No.12CE2005, JSPS, and the RFBR grant N03-03-32699a. The authors thank Dr. M. Kato for the microprobe analysis of compounds **1**–**3**.

[1] H. W. Kroto, J. R. Heath, S. C. O'Brien, R. F. Curl, R. E. Smalley, *Nature* **1985**, *318*, 162.
[2] M. J. Rosseinsky, *J. Mater. Chem*. **1995**, *5*, 1497.
[3] A. L. Balch, M. M. Olmstead, *Chem. Rev.* **1998**, *98*, 2123.
[4] C. A. Reed, R. D. Bolskar, *Chem. Rev*. **2000**, *100*, 1075.
[5] D. V. Konarev, R. N. Lyubovskaya, *Russ. Chem. Rev.* **1999**, *68*, 19.
[6] B. Gotschy, *Fullerene Sci. Technol*. **1996**, *4*, 677.
[7] A. L. Balch, J. W. Lee, B. C. Noll, M. M. Olmstead in *Recent Advances in the Chemistry and Physics of Fullerenes and Related Materiales* (Eds.: K. M. Kadish, R. S. Ruoff), **1994**, *24*, 1231.
[8] J. Stinchcombe, A. Pénicaud, P. Bhyrappa, P. D. W. Boyd, C. A. Reed, *J. Am. Chem. Soc.* **1993**, *115*, 5212.
[9] W. E. Broderick, K. W. Choi, W. C. Wan, *Electrochem. Soc. Proc.* **1997**, *14*, 1102.
[10] a) A. Hönnerscheid, L. Wüllen, M. Jansen, J. Rahmer, M. Mehring, *J. Chem. Phys.* **2001**, *115*, 7161; b) A. Hönnerscheid, R. Dinnebier, M. Jansen, *Acta Crystallogr. Sect. B* **2002**, *58*, 482.
[11] W. C. Wan, X. Liu, G. M. Sweeney, W. E. Broderick, *J. Am. Chem. Soc.* **1995**, *117*, 9580.
[12] P. D. W. Boyd, P. Bhyrappa, P. Paul, J. Stinchcombe, R. D. Bolskar, Y. Sun, C. A. Reed, *J. Am. Chem. Soc.* **1995**, *117*, 2907.
[13] D. V. Konarev, S. S. Khasanov, A. Otsuka, G. Saito, *J. Am.Chem. Soc*. **2002**, *124*, 8520.
[14] C. Bossard, S. Rigaut, D. Astruc, M.-H. Delville, G. Felix, A. F. Bouvier, J. Amiell, S. Flandrois, P. Delhaes, *J. Chem. Soc. Chem. Commun.* **1993**, 333.
[15] A. Pénicaud, J. Hsu, C. A. Reed, A. Koch, K. Khemani, P.-M. Allemand, F. Wudl, *J. Am. Chem. Soc.* **1991**, *113*, 6698.
[16] P.-M. Allemand, K. C. Khemani, A. Koch, F. Wudl, K. Holczer, S. Donovan, G. Grüner, J. D. Thompson, *Science* **1991**, *253*, 301.
[17] A. Izuoka, T. Tachikawa, T. Sugawara, Y. Suzuki, M. Konno, Y. Saito, H. Shinohara, *J. Chem. Soc. Chem. Commun.* **1992**, 1472
[18] G. Saito, T. Teramoto, A. Otsuka, Y. Sugita, T. Ban, M. Kusunoki, K. Sakaguchi, *Synth. Met*. **1994**, *64*, 359.
[19] D. V. Konarev, R. N. Lyubovskaya, N. V. Drichko, E. I. Yudanova, Yu. M. Shul'ga, A. L. Litvinov, V. N. Semkin, B. P. Tarasov, *J. Mater. Chem.* **2000**, *10*, 803.
[20] D. V. Konarev, Yu. V. Zubavichus, E. F. Valeev, Yu. L. Slovokhotov, Yu. M. Shul'ga, R. N. Lyubovskaya, *Synth. Met.* **1999**, *103*, 2364.
[21] D. V. Konarev, A. Yu. Kovalevsky, A. L. Litvinov, N. V. Drichko, B. P. Tarasov, P. Coppens, R. N. Lyubovskaya, *J. Solid State Chem.* **2002**, *168*, 474.
[22] P. D. W. Boyd, M. C. Hodgson, C. E. F. Rickard, A. G. Oliver, L. Chaker, P. J. Brothers, R. D. Bolskar, F. S. Tham, C. A. Reed, *J. Am. Chem. Soc*. **1999**, *121*, 10487.
[23] D. V. Konarev, I. S. Neretin, Yu. L. Slovokhotov, E. I. Yudanova, N. V. Drichko, Yu. M. Shul'ga, B. P. Tarasov, L. L. Gumanov, A. S. Batsanov, J. A. K. Howard, R. N. Lyubovskaya, *Chem. Eur. J.* **2001**, *7*, 2605.
[24] D. M. Eichhorn, S. Yang, W. Jarrell, T. F. Baumann, L. S. Beall, A. J. P. White, D. J. Williams, A. G. M. Barrett, B. M. Hoffman, *J. Chem. Soc. Chem. Commun.* **1995**, 1703.
[25] a) M. M. Olmstead, D. A. Costa, K. Maitra, B. C. Noll, S. L. Phillips, P. M. van Calcar, A. L. Balch, *J. Am. Chem. Soc.* **1999**, *121*, 7090; a) T. Ishii, N. Aizawa, M. Yamashita, H. Matsuzaka, T. Kodama, K. Kikuchi, I. Ikemoto, Y. Iwasa, *J.Chem. Soc. Dalton Trans.* **2000**, 4407.
[26] a) E. I. Yudanova, D. V. Konarev, L. L. Gumanov, R. N. Lyubovskaya, *Russ. Chem. Bull*. **1999**, *48*, 718; b) D. R. Evans, N. L. P. Fackler, Z. Xie, C. E. F. Rickard, P. D. W. Boyd, C. A. Reed, *J. Am. Chem. Soc*. **1999**, *121*, 8466; c) D. V. Konarev, E. I. Yudanova, I. S. Neretin, Yu. L. Slovokhotov, R. N. Lyubovskaya, *Synth. Met.* **2001**, *121*, 1119; d) T. Ishii, R. Kenehama, N. Aizawa, M. Yamashita, H. Matsuzaka, K. Sugiura, H. Miyasaka, T. Kodama, K. Kukuchi, I. Ikemoto, H. Tanaka, K. Marumoto, S. Kuroda, *J. Chem. Soc. Dalton Trans.* **2001**, 2975; e) D. V. Konarev, A. Yu. Kovalevsky, X. Li, I. S. Neretin, A. L. Litvinov, N. V. Drichko, Yu. L. Slovokhotov, P. Coppens, R. N. Lyubovskaya, *Inorg. Chem.* **2002**, *41*, 3638.
[27] a) K. Tashiro, T. Aida, J.-Y. Zheng, K. Kinbara, K. Saigo, S. Sakamoto, K. Yamaguchi, *J. Am. Chem. Soc*. **2000**, *122*, 10704; b) D. Sun, F. S. Tham, C. A. Reed, L. Chaker, M. Burgess, P. D. W. Boyd, *J. Am. Chem. Soc*. **2000**, *122*, 10704; c) J. Y. Zheng, K. Tashiro, Y. Hirabayashi, K. Kinbara, K. Saigo, T. Aida, S. Sakamoto, K. Yamaguchi, *Angew. Chem.* **2001**, *113*, 1909; *Angew. Chem. Int. Ed*. **2001**, *40*, 1857.
[28] D. H. Hochmuth, S. L. J. Michel, A. J. P. White, D. J. Williams, A. G. M. Barrett, B. M. Hoffman, *Eur. J. Inorg. Chem*. **2000**, 593.
[29] S. Valcher, G. Casalbore, M. Mastragostino, *J. Electroanal. Chem*. **1974**, *51*, 226.
[30] D. Dubois, K. M. Kadish, S. Flanagan, R. E. Haufler, L. P. F. Chibante, L. J. Wilson, *J. Am. Chem. Soc.* **1991**, *113*, 4363.
[31] Y. Yoshida, A. Otsuka, O. Drozdova, K. Yakushi, G. Saito, *J. Mater. Chem.*, **2003**, *13*, 252.
[32] D. V. Konarev, S. S. Khasanov, A. Otsuka, Y. Yoshida, G. Saito, *J. Am. Chem. Soc.* **2002**, *124*, 7648.
[33] E. D. Stevens, *J. Am. Chem. Soc.* **1981**, *103*, 5087.
[34] H. P. Fritz, W. Lüttke, H. Stammreich, R. Forneris, *Chem. Ber*. **1959**, *92*, 3246.
[35] T. Picher, R. Winkler, H. Kuzmany, *Phys. Rev. B: Solid State*, **1994**, *49*, 15879.
[36] V. N. Semkin, N. G. Spitsina, S. Krol, A. Graja, *Chem. Phys. Lett.* **1996**, *256*, 616.
[37] V. N. Semkin, N. G. Spitsina, A. Graja, *Chem. Phys. Lett*. **1995**, *233*, 291.
[38] Z. Suo, X. Wei, K. Zhou, Y. Zhang, C. Li, Z. Hu, *J. Chem. Soc. Dalton Trans*. **1998**, 3875.
[39] M. G. Kaplunov, E. V. Golubev, A. V. Kulikov, N. G. Spitsina, *Izv. Acad. Nauk*, *Ser. Khim.* **1999**, 785.
[40] C. Elschenbroich, E. Bilger, J. Koch, *J. Am. Chem. Soc*. **1984**, *106*, 4297.
[41] B. B. Wayland, J. V. Minkiewicz, M. E. Abd-Elmageed, *J. Am. Chem. Soc*. **1974**, *96*, 2795.
[42] A. Pénicaud, A. Peréz-Benítez, R. Escudero, C. Coulon, *Solid State Commun* **1995**, *96*, 147.
[43] M. Rossi, J. P. Glusker, L. Randaccio, M. F. Summers, P. J. Toscano, L. G. Marzilli, *J. Am. Chem. Soc*. **1985**, *107*, 1729.
[44] J. M. Assour, *J. Chem. Phys.* **1965**, *43*, 2477.
[45] T. Nowlin, S. Subramanian, K. Cohn, *Inorg. Chem*. **1972**, *11*, 2907.
[46] B. B. Wayland, L. W. Olson, *J. Am. Chem. Soc*. **1974**, *96*, 6037.
[47] D. M. Guldi, *Chem. Commun*. **2000**, 321.
[48] M. Keshavarz-K, B. Knight, G. Srdanov, F. Wudl, *J. Am. Chem. Soc*. **1995**, *117*, 11371.
[49] J. S. Miller, D. M. O'Hare, A. Chakraborty, A. J. Epstein, *J. Am. Chem. Soc*. **1989**, *111*, 7853.
[50] R. C. Haddon, L. F. Schneemeyer, J. V. Waszczak, S. H. Glarum, R. Tycko, G. Dabbagh, A. R. Kortan, A. J. Muller, A. M. Mujsce, M. J. Rosseinsky, S. M. Zahurak, A. V. Makhija, F. A. Thiel, K. Raghavachari, E. Cockayne, V. Elser, *Nature* **1991**, *350*, 46.
[51] W. Luo, H. Wang, R. Ruoff, J. Cioslowski, S. Phelps, *Phys. Rev. Lett.* **1994**, *73*, 186.
[52] Z. Otwinowski, W. Minor, *Methods Enzymol.* **1997**, 276.
[53] G. M. Sheldrick, SHELX97, University of Göttingen, Germany, **1997**.

Received: October 1, 2002
Revised: February 6, 2003 [F4470]